Liquid fraction in stratiform mixed-phase clouds from *in situ* observations

By FAISAL S. BOUDALA[1]*, GEORGE A. ISAAC[2], STEWART G. COBER[2] and QIANG FU[3]

[1]*Department of Physics and Atmospheric Science, Dalhousie University, Halifax, Canada*
[2]*Cloud Physics and Severe Weather Research Division, Meteorological Service of Canada, Toronto, Canada*
[3]*Department of Atmospheric Sciences, University of Washington, Seattle, USA*

SUMMARY

Liquid fractions in mixed-phase clouds have been analysed using aircraft measurements taken in mid- and high latitude stratiform clouds. The liquid fraction generally increases with temperature but has a minimum at about $-15\,^{\circ}$C, where the maximum ice crystal growth based on vapour deposition would be expected. The mean liquid fraction also depends on total water content. This suggests that segregation of cloud phase based on a simple linear relationship of phase fraction (ice or liquid) with temperature, as is used in some climate models, may be unrealistic. Parametrizations of mean liquid fraction in terms of temperature and total water content, and in terms of temperature alone, have been developed based on data averaged at 10 s resolution (1 km). These parametrizations agree reasonably well with the observations.

KEYWORDS: Cloud phase   Parametrization   Supercooled

1. INTRODUCTION

When supercooled cloud droplets and ice crystals coexist in a given cloud, the ice crystals can grow rapidly to initiate precipitation. This has been theorized by Bergeron (1935). The theory is based on the fact that ice crystals and liquid drops cannot coexist in equilibrium at sub-zero temperatures, due to the fact that the vapour pressure at the surface of ice is smaller than that over liquid drops (Wegener 1911). Observations indicate that supercooled drops may coexist with ice crystals in clouds at temperatures as low as $-40\,^{\circ}$C (Zak 1937; Klinov 1959; Borovikov *et al.* 1963; Sassen 1992; Heymsfield and Miloshevich 1993). The radiative properties of clouds can be altered by the presence of ice crystals (Foot 1988; Sun and Shine 1994). A modelling study by Sun and Shine (1994) shows that the radiative properties of clouds are very sensitive to how the clouds are assumed to be mixed. Generally, a 'mixed-phase cloud' is taken to be a cloud with liquid and ice co-existing. However, ice crystals may be embedded in supercooled liquid layers (e.g. Heymsfield *et al.* 1991), or a glaciated layer may be topped by a supercooled liquid layer (e.g. Cooper and Vali 1981; Hobbs and Rangno 1985). Fu and Hollars (2004) found that mixed-phase clouds on a scale of about 100 m may be composed of liquid droplet and ice particle patches. On a similar scale, Korolev *et al.* (2003) have shown that stratiform clouds are dominated by either ice or liquid phase for temperatures ranging from 0 to $-35\,^{\circ}$C.

Distributions of liquid and glaciated clouds, and the identification of cloud mixing, can be important for parametrization of cloud phase in numerical models, since such sub-scale inhomogeneities are important for the simulation of mixed-phase clouds in models ranging from large-eddy simulations to general circulation models (GCMs). For the scale of a GCM, ensembles of clouds may exist in a mixture of phases at a single grid point. In this study we focus on the liquid water fraction on a scale of ~ 1 km. The liquid fraction (f_{L}) is defined as:

$$f_{\mathrm{L}} = \frac{LWC}{IWC + LWC},\qquad(1)$$

* Corresponding author: Department of Physics and Atmospheric Science, Dalhousie University, Halifax, Nova Scotia, Canada. e-mail: faisalboudala@rogers.com

where *LWC* is the liquid water content and *IWC* is the ice water content. There have been some studies of *LWC* and *IWC* from *in situ* aircraft measurements (e.g. Cober *et al.* 2001; Boudala *et al.* 2002a; Korolev *et al.* 2003). However, there have been few studies of their ratios in mixed-phase clouds (e.g. Isaac and Shemenaur 1979; Moss and Johnson 1994; Bower *et al.* 1996; Cober *et al.* 2001; Korolev *et al.* 2003). Smith (1990) developed a parametrization of liquid fraction as a function of temperature for application in the UK Met Office Atmospheric General Circulation Model. In this scheme, it is assumed that all clouds are liquid at temperatures greater than 0 °C, and are all ice at temperatures lower than −15 °C. Bower *et al.* (1996) have parametrized liquid fraction as a function of temperature for convective and frontal clouds separately, based on limited *in situ* aircraft measurements. The parametrization of liquid fraction has been difficult, mainly because of large uncertainties in the simultaneous measurement of *IWC* and *LWC*, and the identification and separation of cloud water phases. Derivation of *IWC*, based on ice particle spectra measured using two-dimensional (2D) optical array probes such as the PMS (Particle Measuring System) 2D-C and 2D-P, is particularly problematic. This is partly because the circular images of cloud particles can be either water droplets or ice crystals, and small particles (diameter $D < 125$ μm) cannot be reliably identified as ice or liquid on the basis of shape. Another difficulty is how to determine the ice particle mass from 2D images. Tremblay *et al.* (1996) parametrized ice fraction in terms of temperature, total water content (*TWC*), and vertical velocity for application in the Canadian Global Environmental Multiscale model. Their work indicates that a parametrization of liquid fraction as a function of temperature only may not be appropriate. It is worth noting that in their modelling scheme all clouds are assumed to be glaciated for temperatures less than −20 °C, and all are assumed to be liquid for temperatures greater than 0 °C, which may not always be true. Currently there are some bulk cloud microphysical schemes used in GCMs that can estimate the liquid water fraction in a GCM grid cell (e.g. Rotstayn *et al.* 2000; Lohmann and Roeckner 1996). However, these models are based on approximations and they should be validated with direct *in situ* observations. Recent modelling studies by Tremblay *et al.* (2002) and Morrison *et al.* (2003) indicate that one of the major problems in simulating a mixed-phase cloud is predicting the liquid fraction, which is invariably underestimated.

The aim of this work is to develop a parametrization of liquid fraction in terms of temperature and cloud water content based on measurements from stratiform clouds containing an ensemble of phases.

2.   Measurements

The data used in this paper were collected during the five projects described below; in all of these the National Research Council (NRC) Convair-580 aircraft was used. The FIRE Arctic Cloud Experiment (FIRE.ACE) project began in April and ended in July 1998, with the Convair-580 measurements being made in April (Curry *et al.* 2000). The First Canadian Freezing Drizzle Experiment (CFDE I) project was conducted in March 1995, and included numerous flights over Newfoundland and the Atlantic Ocean. The Third Canadian Freezing Drizzle Experiment (CFDE III) started in December 1997 and ended in February 1998; during CFDE III, the aircraft flew over Southern Ontario, Quebec, Lake Ontario and Lake Erie (Cober *et al.* 2001; Isaac *et al.* 2001a). The Alliance Icing Research Study (AIRS) was conducted between 29 November 1999 and 19 February 2000 (Isaac *et al.* 2001b). The Beaufort and Arctic Storms Experiment (BASE) field project was conducted in October 1994 over the Canadian Western Arctic (Gultepe *et al.* 2000).
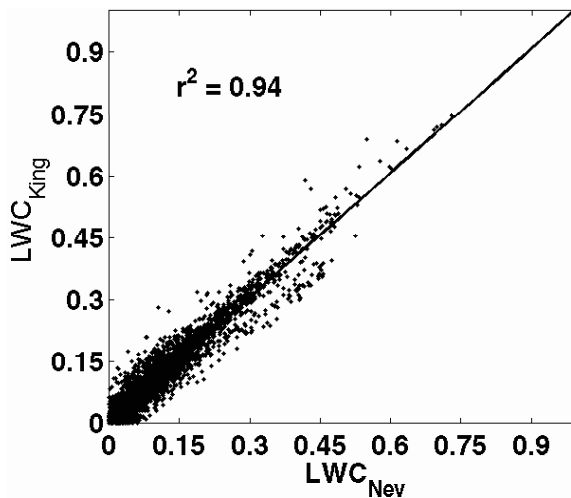
Figure 1.   Liquid water content (*LWC*) measured with the King probe plotted against *LWC* measured with the Nevzorov *LWC* probe. The variance (r^2) is also shown.

The types of instrumentation used in these projects are described in Isaac *et al.* (2001a,b). The instruments used for this work were the King probe which measures *LWC*, Nevzorov *LWC* and *TWC* probes, and the PMS 2D-C and 2D-P probes which measure size, shape and concentration of hydrometers. Temperature was measured with a Rosemount temperature probe.

The 2D-C images were processed following a 'center-in' scheme (Heymsfield and Parrish 1978). This scheme includes all partly imaged particles that have their centres within the sampling area. Their sizes are determined by reconstruction of their shapes assuming a circular geometry (Cober *et al.* 2001). The 2D-P images were processed following an 'entire-in' scheme (Knollenberg 1970). This method is based on ignoring any particle that occludes either end element of the photodiode array.

Korolev *et al.* (1998) describe the Nevzorov TWC/LWC probe. The probe has two separate sensors, one for *TWC* and the other for *LWC* measurements. Comparison measurements made with the Nevzorov and similar types of probes in high speed wind-tunnel experiments suggest that the probe can measure *LWC* and *TWC* within an accuracy of 15%, and the sensitivity of the instrument is estimated to be in the range of 0.003 to 0.005 gm^{-3}. The Nevzorov LWC probe also responds to ice crystals in glaciated or mixed-phase clouds, and this response is estimated to be about 10–15% of the *IWC* measurements (Cober *et al.* 2001; Korolev *et al.* 2003) at the typical speeds of the Convair-580. For the mixed-phase cloud case, the Nevzorov *LWC* data have been corrected following Korolev *et al.* (2003). The threshold value for the Nevzorov *TWC* measurements was assumed to be 0.01 gm^{-3}, and only data with $TWC > 0.01$ gm^{-3} were used for developing the parametrization.

King *et al.* (1978) describe the King probe. It is a hot wire probe like the Nevzorov probe but with a lower sensitivity of 0.02 gm^{-3}. In this study, the King probe measurements were used for comparisons and the Nevzorov probe measurements were used for development of the parametrization.

Figure 1 shows comparisons of *LWC* measured in mixed-phase clouds using the Nevzorov and King LWC probes during the CFDE I, CFDE III, and AIRS projects. The *LWC* values measured using the King probe (LWC_K) and the Nevzorov probe
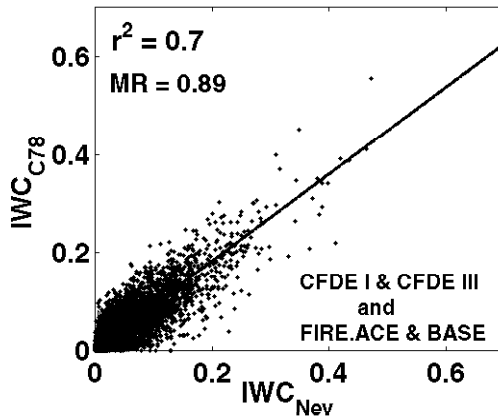
Figure 2. Ice water content (*IWC*) derived from PMS two-dimensional images (*IWC$_{C78}$*) compared with *IWC* calculated from the Nevzorov TWC/LWC (total water content/liquid water content) probes. See text for further details.

(*LWC$_{Nev}$*) correlate well, with a correlation coefficient (*r*) near 0.97. A similar comparison based on projects CFDE I and CFDE III in liquid clouds was reported by Cober *et al.* (2001).

Figure 2 shows a comparison of *IWC* derived from 30 s averaged particle spectra measured in mixed-phase cloud using PMS 2D-C and 2D-P probes during the CFDE I, CFDE III, FIRE.ACE and BASE projects. The *IWC* referred to here as *IWC$_{Nev}$* was calculated from the Nevzorov probe as (*TWC$_{Nev}$* − *LWC$_{Nev}$*). The *IWC$_{C78}$* values were derived from PMS 2D-C and 2D-P data using the Cunningham (1978) coefficients as described in Boudala *et al.* (2002a). *IWC$_{C78}$* and *IWC$_{Nev}$* generally show a reasonable correlation (coefficient *r* = 0.84) with a mean ratio (*MR*) of 0.9. The derived *IWC* from spectra underestimate the measured *IWC* on average by about 10%, probably because small particles are not included in the calculation. Boudala *et al.* (2002a) found that *IWC$_{C78}$* was ≈20% lower than *IWC$_{Nev}$* for cloud regions that were glaciated. In addition to missing small ice crystals, a number of other reasons can affect this percentage in the case of mixed-phase clouds.

3. LIQUID FRACTION

Table 1 shows the average *LWC*, *IWC*, *TWC*, and f_L values for every 2 degC temperature interval for data averaged over 10 s (or approximately 1 km in aircraft path length) for all clouds. The standard deviation (*SD*) of f_L, the number of averaged data points for each temperature interval, and the mean temperature within the temperature interval are also given. Table 1 includes the collective datasets from CFDE I, CFDE III, FIRE.ACE, and AIRS, corrected as described in section 2. The *SD* for individual points can be smaller or larger than the mean value. The mean *SD* for each project ranged from 0.21 to 0.39. The lowest value of the mean *SD* was for FIRE.ACE. The averaged liquid fraction for each individual field project is plotted against temperature in Fig. 3. Generally f_L increases with increasing temperature, except near −15 °C. The most striking similarity among all projects is the minimum in f_L that occurred between about −20 and −10 °C. In the case of f_L based on all the data, this minimum is near −15 °C as shown in Fig. 4(a), which plots the mean and SD values of f_L versus

TABLE 1.   AVERAGE WATER CONTENTS AND LIQUID FRACTIONS AVERAGED OVER ALL CLOUDS

Liquid water content LWC (g m^{-3})	Ice water content IWC (g m^{-3})	Total water content TWC (g m^{-3})	Liquid fraction f_L	Standard deviation of f_L	Mean temperature T (°C)	Number of data points
0.115	0.032	0.147	0.733	0.356	−1.1	4247
0.102	0.038	0.141	0.675	0.388	−3.0	5800
0.084	0.039	0.122	0.621	0.422	−5.0	5582
0.075	0.039	0.114	0.566	0.433	−7.0	6218
0.081	0.028	0.109	0.586	0.423	−9.0	4052
0.070	0.034	0.105	0.470	0.426	−11.0	3058
0.046	0.048	0.095	0.365	0.384	−13.0	2306
0.021	0.038	0.059	0.266	0.304	−14.9	1353
0.021	0.035	0.056	0.355	0.371	−17.0	1340
0.034	0.023	0.057	0.503	0.412	−19.0	1268
0.023	0.020	0.043	0.417	0.379	−20.9	1180
0.017	0.029	0.047	0.321	0.353	−22.8	307
0.008	0.025	0.033	0.226	0.249	−24.9	252
0.016	0.032	0.048	0.270	0.305	−27.1	288
0.014	0.026	0.040	0.242	0.297	−28.9	439
0.016	0.016	0.032	0.238	0.282	−30.6	77
0.003	0.015	0.019	0.139	0.232	−33.2	54
0.002	0.017	0.019	0.119	0.164	−34.9	33
0.001	0.015	0.016	0.080	0.054	−37.2	58
0.000	0.011	0.011	0	0	−38.8	7

Combined CFDE I, CFDE III, FIRE.ACE and AIRS, 10 s averaged data binned at every 2 degC interval. See text for details.
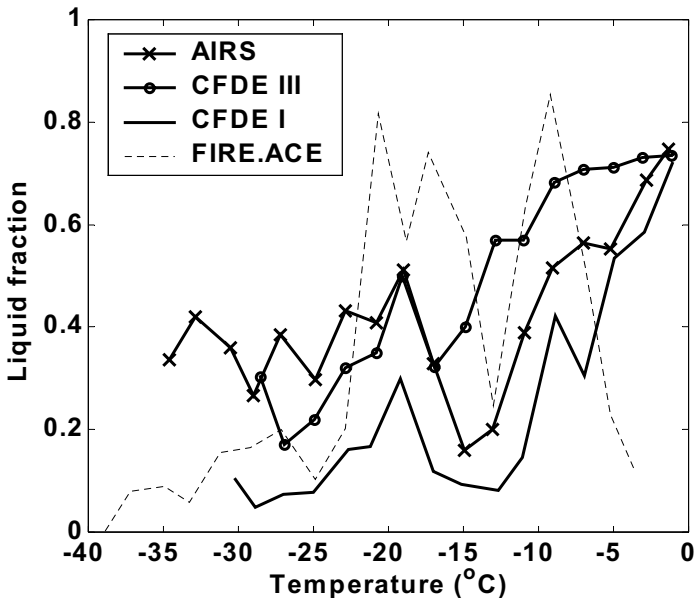

Figure 3.   The 10 s averaged liquid fraction for every 2 degC temperature interval plotted against temperature for each project. See text for details.

temperature. Figure 4(b) shows the 25, 50 and 75% values of liquid fraction plotted against temperature. The minimum near −15 °C in f_L is also clearly evident using this method of presenting the data. Under laboratory conditions, the maximum ice crystal growth rate occurs near −15 °C (Fukuta 1969; Takahashi and Fukuta 1988; Pruppacher and Klett 1997; Fukuta and Takahashi 1999) which may partially explain the minimum in liquid fraction around −15 °C.
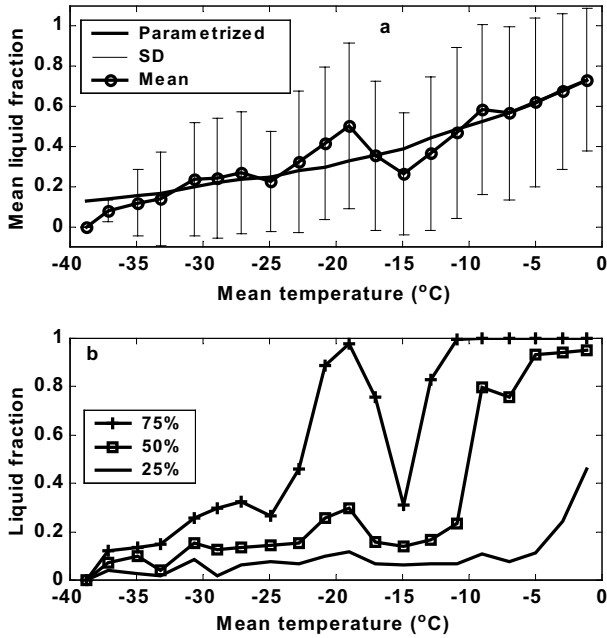
Figure 4. The 10 s averaged liquid fraction for every 2 degC temperature interval plotted against temperature for all data given in Table 1: (a) The mean, standard deviation (SD) bars, and a parametrization using Eq. (2); (b) 75%, 50%, and 25% percentiles. See text for further details.

4. PARAMETRIZATION OF LIQUID FRACTION

As indicated in Fig. 3, there is no systematic dependence of f_L on latitude; therefore, it is both useful and justifiable to develop a parametrization of f_L based on the entire dataset given in Table 1. Figure 5 shows 10 s averaged data binned by temperature and *TWC* (Fig. 5(a)), and by temperature and *LWC* (Fig. 5(b)). On average, f_L increases with both increasing temperature and *TWC* if the minimum near $-15\,°\text{C}$ is ignored. For given *TWC*, f_L approximately increases with increasing temperature. When temperature increases, both *TWC* and *LWC* increase, but the rate of increase of *LWC* is faster than the increase in *TWC*. The liquid fraction increases with increasing *LWC* as expected. It is interesting, however, to note that for a given *LWC*, f_L approximately increases with decreasing temperature for lower *LWCs*, but remains approximately constant for higher *LWCs*. The increasing tendency of f_L at lower *LWCs* may be associated with the fact that generally *TWC* decreases with decreasing temperature and the ice mass also decreases with decreasing temperature (e.g. Boudala *et al.* 2002a). Therefore, a parametrization of f_L as a function of both temperature and *TWC* or *LWC* seems to be more reasonable as suggested by Tremblay *et al.* (1996) and Boudala *et al.* (2002b). Note that Tremblay *et al.* have included vertical velocity in their parametrization based on some physical arguments. In this work, however, this parameter is not included because of the absence of accurate measurements of vertical velocity. However, vertical velocity is also expected to be correlated with *TWC* (Srivastava 1967; Heymsfield 1977). A simple parametrization similar to the one proposed by Boudala *et al.* (2002b), given in the form:

$$f_L(T, TWC) = \beta_1 TWC^{\beta_2} \exp(\beta_3 T) \left| \begin{array}{l} \beta 1 = 1.0 \\ \beta 2 = 0.141 \\ \beta 3 = 0.037 \end{array} \right., \tag{2}$$
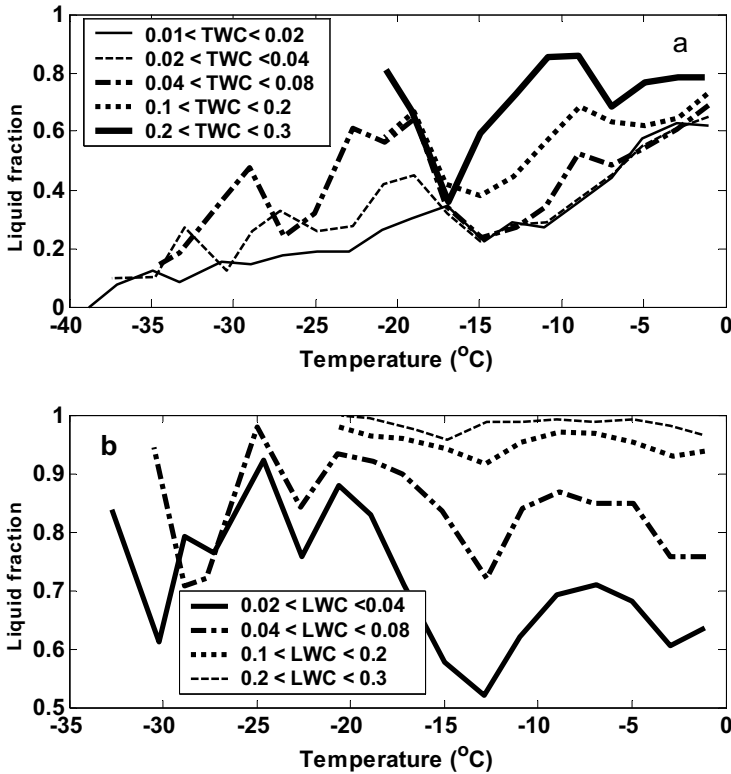
Figure 5. The measured liquid fraction for every 2 degC temperature interval plotted against temperature for all data given in Table 1: (a) binned by temperature and total water content (*TWC*) plotted against mean temperature, and (b) binned by temperature and liquid water content (*LWC*) plotted against mean temperature. See text for further details.

adequately captures the variability of the mean f_L with $r = 0.94$ (see Fig. 6). However, this parametrization does not capture the liquid fraction minimum near $-15\,°C$, and also slightly overestimates the mean liquid fraction at temperatures near $-38.5\,°C$ (see Fig. 4(a)). These problems can be resolved by using a more complicated polynomial function in a form:

$$f_L(T, TWC) = \left(c - \frac{0.15 IWC(T)}{TWC}\right)^{2.5} (a_{10}T^{10} + a_9 T^9 + a_8 T^8 + a_7 T^7 + a_6 T^6$$
$$+ a_5 T^5 + a_4 T^4 + a_3 T^3 + a_2 T^2 + a_1 T + a_0), \qquad (3)$$

where T is temperature in $°C$. As indicated in Fig. 7, the liquid fraction calculated using this function correlated well with observation with $r = 0.99$. The function $IWC(T)$ in Eq. (3) represents the measured IWC based on all projects (see Table 1) and is parametrized using a function in a form (see Fig. 8):

$$IWC(T) = d_8 T^8 + d_7 T^7 + d_6 T^6 + d_5 T^5 + d_4 T^4 + d_3 T^3 + d_2 T^2 + d_1 T + d_0, \quad (4)$$

where the coefficients a_n and d_n are given in Table 2. The constant, c, is given by a relation $c = \max(1, IWC(T)/TWC)$. It is worth noting from Fig. 8 that the mean *IWC* is a maximum near $-15\,°C$ where the liquid fraction is minimum. In glaciated ice clouds, in contrast to the mixed-phase clouds of Fig. 8, it has been shown that *IWC*
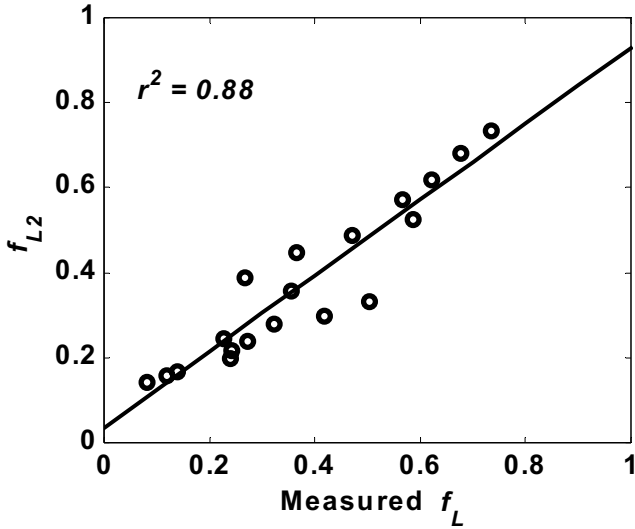
Figure 6. The parametrized liquid fraction (f_L) using Eq. (2) plotted against observations. The variance r^2 is also shown. See text for further details.
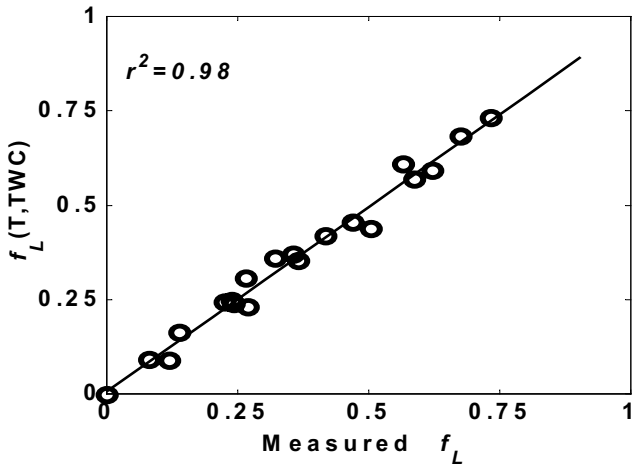

Figure 7. The liquid fraction (f_L) plotted against the observations. The variance r^2 is also shown. See text for further details.

increases with increasing temperature (Heymsfield and Platt 1984; Stephens *et al.* 1990; McFarquhar and Heymsfield 1997; Boudala *et al.* 2002a).

Figure 9 shows the parametrized f_L based on Eq. (3) plotted against temperature for a given *TWC*. The parametrization captures well the liquid fraction minimum near −15 °C. For a given temperature, the liquid fraction increases with increasing *TWC*. Based on the Tremblay *et al.* (1996) parametrization, for a given *TWC* the proportion of supercooled liquid water generally decreases with decreasing temperature. However, this is not always true based on the observations shown in Fig. 5. The ice fraction $1 - f_L$ generally decreases with increasing *TWC*, and this is also contrary to the finding of Tremblay *et al.* (1996).
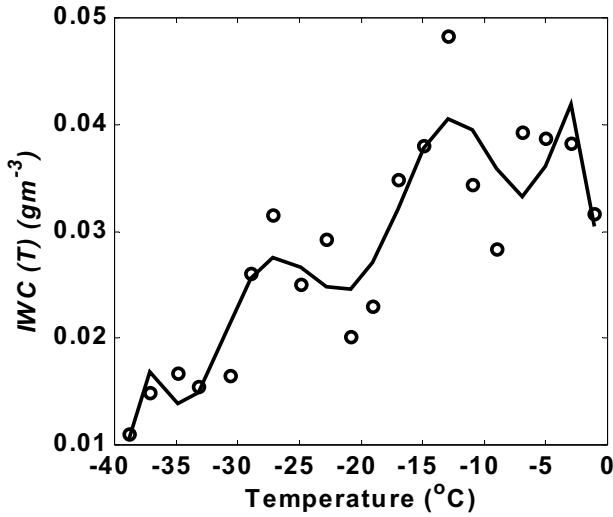
Figure 8.   The mean ice water content (*IWC*) from all projects and the parametrization (open circles) plotted against temperature (*T*).

TABLE 2.   COEFFICIENTS FOR THE LIQUID FRACTION PARAMETRIZATIONS

$f_L(T) = \sum\limits_{n=0}^{11} c_n T^n$	$a_{\text{iwc}}(T) = \sum\limits_{n=0}^{8} d_{n-1} T^{n-1}$	$f_L(T, TWC) = \left(c - \dfrac{0.15 a_{\text{iwc}}}{TWC}\right)^{2.5} \sum\limits_{n=0}^{8} a_n T^n$
$c_{10} = -3.003\,236, e - 12$	$d_8 = -2.042137, e - 11$	$a_{10} = -3.452\,805, e - 12$
$c_9 = -5.864\,285, e - 10$	$d_7 = -3.271\,094, e - 9$	$a_9 = -6.733\,281, e - 10$
$c_8 = -4.856\,203, e - 8$	$d_6 = -2.137\,06, e - 7$	$a_8 = -5.567\,808, e - 8$
$c_7 = -2.218\,146, e - 6$	$d_5 = -7.309\,977, e - 6$	$a_7 = -2.539\,095, e - 6$
$c_6 = -6.084\,225, e - 5$	$d_4 = -1.397\,167, e - 4$	$a_6 = -6.951\,845, e - 5$
$c_5 = -1.021\,934, e - 3$	$d_3 = -1.474\,68, e - 3$	$a_5 = -1.165\,2409, e - 3$
$c_4 = -1.026\,042, e - 2$	$d_2 = -7.997\,589, e - 3$	$a_4 = -1.167\,238, e - 2$
$c_3 = -5.726\,352, e - 2$	$d_1 = -1.904\,455, e - 2$	$a_3 = -6.498\,436, e - 2$
$c_2 = -1.512\,94, e - 1$	$d_0 = +2.276\,435, e - 2$	$a_2 = -1.712\,1696, e - 1$
$c_1 = -9.442\,889, e - 2$		$a_1 = -1.096\,085, e - 1$
$c_0 = +8.687\,381, e - 1$		$a_0 = +8.632\,512, e - 1$

See text for details.

It should be mentioned that the threshold value for *TWC* measurements used for developing this parametrization has been taken to be 0.01 gm^{-3}, because of the uncertainty of the measurements discussed earlier. Therefore, the accuracy of this parametrization for *TWC* of less than 0.01 gm^{-3}, cannot be justified based on the data.

When the *TWC* or *IWC* data are not available, the liquid fraction can be estimated by a polynomial function as

$$f_L(T) = c_8 T^8 + c_7 T^7 + c_6 T^6 + c_5 T^5 + c_4 T^4 + c_3 T^3 + c_2 T^2 + c_1 T + c_0, \quad (5)$$

where the coefficients c_n are given in Table 2. This parametrization correlated quite well with observations, with $r = 0.98$, which is identical to the value shown in Fig. 7.

Although the parametrizations given in Eqs. (3) and (5) correlated remarkably well with the mean liquid fraction, fitting data to high-order polynomials can be a significant source of numerical error and instability, thus they should be applied with caution.
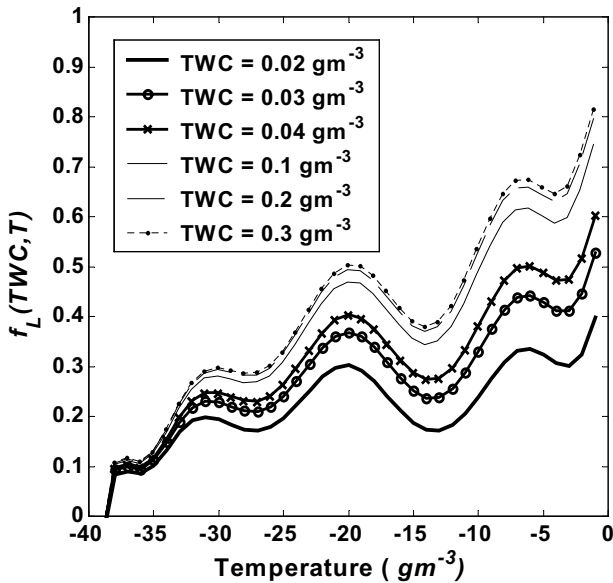
Figure 9. The liquid fraction (f_L) parametrized as a function of temperature (T) and total water content (TWC) using Eq. (3), plotted against temperature for arbitrary TWC intervals as shown.

These parametrizations are only applicable for a temperature range $0 > T \geqslant -38.5\,°C$. For $T \geqslant 0\,°C$ and $T < -38.5°C$ the liquid fraction may be assumed to be unity and zero, respectively. In the presence of falling ice particles at the base of cloud, liquid fraction may not be unity near $0\,°C$, but the assumption is not unreasonable. It should be noted here that if any of the parametrizations in this paper are applied to 1 or 10 s averaged datasets without temperature averaging, the correlation coefficients are significantly lower (close to 0.4). Therefore, these parametrizations are applicable for mean atmospheric conditions.

5. SUMMARY AND CONCLUSIONS

Liquid fractions averaged over 10 s intervals in stratiform clouds were analysed from more than 37 918 *in situ* data points (representing approximately 1 km path lengths) in geographical regions between 72°N and 45°N. The cloud liquid fraction observed (f_L) showed no systematic dependence on latitude. The dominant features observed in all field projects were that the mean f_L generally increased with temperature and TWC for temperatures colder and warmer than $-15\,°C$, with the existence of a minimum near $-15\,°C$ where the maximum ice crystal growth based on vapour deposition would be expected. Parametrizations of f_L as a function of T and TWC, and T alone have been developed based on the observed data. The parametrizations correlate well with the observed f_L, and two of them capture the observed minimum in f_L between -10 and $-20\,°C$. The developed parametrizations based on T and TWC also predict that f_L increases with increasing TWC. Parametrization of mixed-phase cloud processes is a difficult problem. The data analysed and presented in this work can be useful for parametrizing f_L or validating simulations within cloud-resolving models and GCMs.

REFERENCES

Bergeron, T.	1935	'On the physics of cloud and precipitation'. Pp. 156–178 in Proceedings of the fifth assembly of IUGG, Vol. 2, Lisbon, Portugal
Boudala, F. S., Isaac, G. A., Fu, Q. and Cober, S. G.	2002a	Parametrization of effective ice particle sizes for high latitude clouds. *Int. J. Climatol.*, **22,** 1267–1284
Boudala, F. S., Isaac, G. A., Cober, S. G., Fu, Q. and Korolev, A. V.	2002b	'Parametrization of liquid fraction in terms of temperature and cloud water content in stratiform mixed-phase clouds'. In Proceedings of the eleventh conference on cloud physics, June 3–7, Ogden, UT. American Meteorological Society, Boston USA
Bower, K., Moss, S. J., Johnson, D. W., Choularton, T. W., Latham, J., Brown, P. R. A., Blyth, A. M. and Cardwell, J.	1996	A parametrization of ice water content observed in frontal and convective clouds. *Q. J. R. Meteorol. Soc.*, **122,** 1815–1844
Borovikov, A. M., Gaivoronskii, I. I., Zak, E. G., Kostarev, V. V., Mazin, I. P., Minervin, V. E., Khrgian. A. Kh. and Shmeter, S. M.	1963	'Clouds physics'. Israel Program for Scientific Translation. Available from US Dept. of Commerce, Washington, DC, USA
Cober, S. G., Isaac, G. A., Korolev, A. V. and Strapp, J. W.	2001	Assessing cloud-phase conditions. *J. Appl. Meteorol.*, **40,** 1967–1983
Cooper, W. A. and Vali, G.	1981	The origin of ice in mountain cap clouds. *J. Atmos. Sci.*, **38,** 1244–1259
Cunningham, M. R.	1978	'Analysis of particle spectral data from optical array (PMS) 1D and 2D sensors'. Pp. 345–350 in proceedings of the American Meteorological Society, fourth symposium on meteorological observing instruments. Denver, USA, April 10–14 1978. American Meteorological Society, Boston, USA
Curry, J. A., Hobbs, P. V., King, M. D., Randall, D. A., Minnis, P., Isaac, G. A., Pinto, J. O., Uttal, T., Bucholtz, A., Cripe, D. G., Gerber, H., Fairall, C. W., Garrett, T. J., Hudson, J., Intrieri, J. M., Jakob, C., Jensen, T., Lawson, P., Marcotte, D. L., Nguyen, L., Pilewskie, P., Rangno, A., Rogers, D., Strawbridge, K. B., Valero, F. P. J., Williams, A. G. and Wylie, D.	2000	FIRE Arctic Clouds Experiment. *Bull. Am. Meteorol. Soc.*, **81,** 5–29

Foot, J. S.   1988   Some observation of optical properties of clouds. II Cirrus. *Q. J. R. Meteorol. Soc.*, **114,** 145–164

Fu, Q. and Hollars, S.   2004   Testing mixed-phase cloud water vapor parameterization with SHEBA/FIRE_ACE observations. *J. Atmos. Sci.*, in press

Fukuta, N.   1969   Experimental studies of the growth of small ice crystal. *J. Atmos. Sci.*, **26,** 522–531

Fukuta, N. and Takahashi, T.   1999   The growth of atmospheric ice crystals A summary of findings in vertical supercooled cloud tunnel studies. *J. Atmos. Sci.*, **56,** 1963–1979

Gultepe, I., Isaac, G. A., Hudak, D.,   2000   Dynamical and microphysical characteristics of Arctic clouds
Nissen, R. and Strapp, J. W.   during BASE. *J. Climate*, **13,** 1225–1254

Heymsfield, J. A.   1977   Precipitation development in stratiform ice clouds: A microphysical and dynamical study. *J. Atmos. Sci.*, **34,** 367–381

Heymsfield, A. J. and   1993   Homogenous ice nucleation and supercooled liquid water in
Miloshevich, M. L.   orographic wave clouds. *J. Atmos. Sci.*, **50,** 2335–2353

Heymsfield, A. J. and Parrish, J. L.   1978   A computational technique for increasing effective sampling volume of the PMS two dimensional particle size spectrometer. *J. Appl. Meteorol.*, **17,** 1566–1572

Heymsfield, A. J. and   1984   Parametrization of particle size spectrum of ice clouds in terms
Platt, C. M. R.   of ambient temperature and ice water content. *J. Atmos. Sci.*, **41,** 846–855

Heymsfield, A. J.,   1991   Observational and theoretical study of high supercooled altocu-
Miloshevich, M. L.,   mulus. *J. Atmos. Sci.*, **48,** 923–945
Slingo, A., Sassen, K. and
Starr, D.

Hobbs, P. V. and Rangno, A. L.   1985   Ice particle concentrations in clouds. *J. Atmos. Sci.*, **42,** 2523–2549

Isaac, G. A. and Schemenauer, R. S.   1979   Large particles in supercooled regions of northern Canadian cumulus clouds. *J. Appl. Meteorol.*, **18,** 11056–11065

Isaac, G. A., Cober, S. G.,   2001a   Recent Canadian research on aircraft in-flight icing. *Can.
Strapp, J. W., Korolev, A. V.,   Aeronaut. Space J.*, **47,** 213–221
Tremblay, A. and Marcotte, D.

Isaac, G. A., Cober, S. G.,   2001b   'Preliminary results from the Alliance Icing Research Study
Strapp, J. W., Hudak, D.,   (AIRS)'. Proceedings of the 39th Aerospace sciences
Ratvasky, T. P.,   meeting and exhibit, Reno, Nevada, 8–11 January 2001.
Marcotte, D. L. and Fabry, F.   American Institute of Aeronautics and Astronautics 2001-0393,

King, W. D., Parkin, D. A. and   1978   A hot wire liquid water device having fully calculable response
Handsworth, R. J.   characteristics. *J. Appl. Meteorol.*, **17,** 1809–1913

Klinov, F. Y.   1959   On supercooled water in the atmosphere. *Izv Geophys. Ser.*, 1430–1431

Knollenberg, R. G.   1970   The optical array: An alternative to scattering or extinction for airborne particle size determination. *J. Appl. Meteorol.*, **9,** 86–103

Korolev, A. V., Strapp, W. J.,   1998   The Nevzorov airborne hot wire LWC–TWC probe: Principle of
Isaac, G. A. and   operation and performance. *J. Atmos. Oceanic Technol.*, **15,**
Nevzorov, A. N.   1495–1510

Korolev, A. V., Isaac, G.,   2003   Microphysical characterization of mixed phase clouds. *Q. J. R.
Cober, S. G., Strapp, J. W. and   Meteorol. Soc.*, **129,** 39–65
Hallett, J.

Lohmann, U. and Roeckner, E.   1996   Design and performance of a new cloud microphysics scheme developed for ECHAM general circulation model. *Clim. Dyn.*, **12,** 557–572

McFarquhar, G. M. and   1997   Parametrization of tropical cirrus ice crystal size distribution
Heymsfield, A. J.   and implication for radiative transfer: Results from CEPEX. *J. Atmos. Sci.*, **54,** 2187–2200

Morrison, H., Shupe, M. D. and   2003   The modeling of clouds observed at SHEBA using a bulk micro-
Curry, J. A.   physics parametrization implemented into a single-column model. *J. Geophys. Res.*, **108,** 4255–4271

Moss, S. J. and Johnson, D. W.   1994   Aircraft measurements to validate and improve numerical models: Parametrizations of ice to water ratios in clouds. *Atmos. Res.*, **34,** 1–25

Pruppacher, H. R. and Klett, J. D.   1997   *Microphysics of clouds and precipitation*. Kluwer Academic Publisher, London, UK

Rotstayn, D. L., Ryan, B. F. and Katzfey, J. J.   2000   A scheme of calculation of liquid fraction in mixed phase stratiform clouds in large scale models. *Mon. Weather Rev.*, **128,** 1070–1087

Sassen, K.   1992   Evidence of liquid phase cirrus cloud formation from volcanic aerosols: Climate implications. *Science*, **257,** 516–519

Smith, R. N. B.   1990   A scheme for predicting clouds and their water content in a general circulation model. *Q. J. R. Meteorol. Soc.*, **116,** 435–460

Srivastava, C. R.   1967   A study of the effect of precipitation on cumulus dynamics. *J. Atmos. Sci.*, **24,** 36–45

Stephens, G. L., Tsay, S. C., Stackhouse, P. W. and Flatau, P. J.   1990   Relevance of micro-physical and radiative properties of cirrus clouds to climate and climatic feedback. *J. Atmos. Sci.*, **47,** 1742–1753

Sun, Z. and Shine, K. P.   1994   Studies of radiative properties of ice and mixed phase clouds. *Q. J. R. Meteorol. Soc.*, **120,** 111–137

Takahashi, T. and Fukuta, N.   1988   Supercooled cloud tunnel studies in the growth of snow crystal between $-4\,°C$ and $-20\,°C$. *J. Meteorol. Soc. Jpn*, **66,** 841–855

Tremblay, A., Glazer, A., Yu, W. and Benoit, R.   1996   A mixed phase cloud scheme based on a single prognostic equation. *Tellus*, **48A,** 483–500

Tremblay, A., Vaillancourt, P. A., Cober, S. G., Glazer, A. and Isaac, G. A.   2002   Improvements of a mixed-phase cloud scheme using aircraft observations. *Mon. Weather Rev.*, **130,** 672–686

Wegener, A.   1911   *Thermodynamick der Atmosphare*. J. A. Barth. Leipzig, Germany

Zak, E. G.   1937   The characterization of frontal clouds using aircraft sounding. *Soviet Meteorol. and Hydrol.*, **8,** 14–28